

# Performance Test and Component Characteristics Evaluation of a Micro Gas Turbine

**Jong Joon Lee, Jae Eun Yoon**

Graduate School, Inha University,  
253 Yonghyun-Dong, Nam-Gu, Incheon 402-751, Korea

**Tong Seop Kim\***

Department of Mechanical Engineering, Inha University,  
253 Yonghyun-Dong, Nam-Gu, Incheon 402-751, Korea

**Jeong L. Sohn**

School of Mechanical and Aerospace Engineering, Seoul National University,  
Seoul 151-742, Korea

This study aims to analyze engine performance and component characteristics of a micro gas turbine based on detailed measurement of various parameters. A test facility to measure performance of a micro gas turbine was set up and performance parameters such as turbine exit temperature, exhaust gas temperature, engine inlet temperature, compressor discharge pressure and temperature, and fuel and air flow rates were measured. The net gas turbine performance (power and efficiency based on the gas turbine shaft end) was isolated and analyzed. With the aid of measurement based simulation, component characteristic parameters such as turbine inlet temperature, compressor efficiency, turbine efficiency and recuperator effectiveness were estimated. Behaviors of the estimated characteristic parameters with operating condition change were examined and sensitivities of estimated parameters to the measured parameters were analyzed.

**Key Words :** Micro Gas Turbine, Performance Test, Performance Parameters, Characteristic Parameters, Optimal Solution, Sensitivity

## Nomenclature

CDT : Compressor discharge temperature [K]  
EGT : Exhaust gas temperature [K]  
 $h$  : Specific enthalpy [kJ/kg]  
LHV : Lower heating value [kJ/kg]  
MGT : Micro gas turbine  
 $\dot{m}$  : Mass flow rate [kg/s]  
N : Shaft speed [rpm]  
 $P$  : Pressure [kPa]  
PR : Pressure ratio

RMS : Root mean square deviation  
 $T$  : Temperature [K]  
TET : Turbine exit temperature [K]  
TIT : Turbine inlet temperature [K]  
 $\dot{W}$  : Power [kW]  
 $\delta$  : Deviation  
 $\eta$  : Efficiency, effectiveness  
 $\eta_{th}$  : Thermal efficiency at shaft end

## Subscripts

0-8 : Location  
a : Air  
c : Compressor  
f : Fuel  
gen : Generator  
in : Inlet  
m : Measurement

\* Corresponding Author,

**E-mail :** kts@inha.ac.kr

**TEL :** +82-32-860-7307; **FAX :** +82-32-868-1716

Department of Mechanical Engineering, Inha University,  
253 Yonghyun-Dong, Nam-Gu, Incheon 402-751,  
Korea. (Manuscript **Received** May 16, 2006; **Revised**  
November 4, 2006)

max : Maximum  
 out : Outlet  
 rec : Recuperator  
 ref : Reference  
 s : Isentropic  
 sh : Shaft  
 sim : Simulation  
 t : Turbine

## 1. Introduction

Recent attention for the distributed power generation systems has promoted development effort for various small power sources including conventional heat engines and renewable power generators. Among others, the micro gas turbine (MGT) is considered to be one of the prospective candidates considering technical maturity and environment friendliness. Micro gas turbines are defined as small gas turbines, usually less than 200 kW (Rodgers et al., 2001). The maximum temperature (turbine inlet temperature, TIT) of micro gas turbines is limited to far less than those of large gas turbines because using hot section cooling is not feasible. In addition, their pressure ratios are also sufficiently low. Thus, adopting a recuperator is inevitable to overcome efficiency limitation. Currently available MGTs are designed with TIT of 800 to 900°C and pressure ratio of 3 to 5, and their efficiencies are 25 to 30 percent. Endeavors are still being made to develop more efficient and power upgraded versions. Thermal efficiency of 40 percent is the current goal of micro gas turbine developers (US Department of Energy, 2000). There exist many important factors in the development of micro gas turbines, such as designing both efficient and cost-effective compressor and turbine, low emission combustor and robust engine control system, and so on. Technical issues are well summarized in the literature (Simon and Jiang, 2003). In particular, designing a compact and efficient recuperator is deemed to be the most critical considering its critical role in engine performance (McDonald, 2000; McDonald and Rodgers, 2005). Near 40% efficiency, based on currently available micro gas turbines, is also possible by a combined cycle (Lee and Kim, 2006). The re-

cuperated cycle gas turbine exhibits unique part load performance characteristics in comparison with the simple cycle gas turbine due to the existence of the recuperation process. It needs a unique operating strategy such as variable speed control to have good partial load performance (Kim and Hwang, 2006).

Performance diagnostics of micro gas turbines has not been as popular as that of conventional gas turbines. However, as the working hours accumulate, performance of the micro gas turbine also degrades. Therefore, prediction and prevention of the performance degradation of micro gas turbines through appropriate diagnosis will be as important as in conventional gas turbines. The unique features of the micro gas turbine, such as using the recuperator and adopting the digital power control covering a wide operating range in terms of shaft speed, make the performance diagnostics challenging. Recently, a few studies have been reported on the subject of performance test and basic diagnostics. Small jet engines are mostly used in fundamental studies (Yin and Huang, 2003; Davison and Birk, 2004). Reports on performance test of an industrial micro gas turbine for commercial development (Shibata et al., 2003) and prediction of the operating behavior of a commercial micro gas turbine (Chiang et al., 2004) are also available.

For a successful engine diagnosis, information of exact reference data (characteristic parameters) of all major components must be present at first. This study aimed to obtain component characteristic parameters of a micro gas turbine using detailed measurement. A test facility for a commercial micro gas turbine generator has been set up, with various measurements embedded. First, performance of the entire engine was evaluated for a wide operation range. Then, an analysis method, based on optimal matching between measured performance data and simulation results, was used to estimate component characteristic parameters such as compressor and turbine efficiencies, recuperator effectiveness as well as the unmeasured turbine inlet temperature. Sensitivities of estimated parameters to the measured parameters were also analyzed.

## 2. Experiment and Analysis

### 2.1 Micro gas turbine

The micro gas turbine used in this work is a 30 kW class engine, which consists of a single stage centrifugal compressor, a single stage radial turbine, an annular combustor and a primary surface recuperator wrapped around the core engine. The compressor and the turbine are arranged on a single shaft, of which the full speed is 96,000 rpm. This engine adopts air bearings. It also adopts a high speed generator of permanent magnet type, which generates high frequency electricity. The generator is located at the cold end of the shaft (i.e. in front of the compressor) and cooled by the air flowing into the compressor. The generator acts as a starting motor as well. The high speed generator gets rid of the conventional gear box and makes the system compact. To convert the high frequency electricity into the low frequency electricity, a digital power controller (DPC) is equipped. Another important feature regarding the off-design operation of the engine is that the shaft speed changes during power variation. At any speed, only a single operation condition (i.e., single power) exists, which satisfies a specific turbine exit temperature. Therefore, full power is available at the maximum speed (96,000 rpm). Of course, the exact operating condition and the corresponding power vary with ambient condition. This option has been proved to provide far improved part load efficiency of the recuperated cycle gas turbines in comparison with the fuel only control because the resulting high turbine exit temperature enables more effective utilization of the heat recovery at the recuperator (Kim and Hwang, 2006). The variable frequency due to the shaft speed change is converted into the constant low frequency (60 Hz) by the digital power controller.

A fuel compressor, equipped in the generator system, boosts the low pressure natural gas (4,000 mmH<sub>2</sub>O) up to the injection pressure. The embedded control system of the generator set provides several measured parameters such as shaft speed and temperatures at turbine exhaust and

compressor inlet. These temperatures are not easy to measure additionally since the measuring points are located inside the engine casing. Therefore, these temperature data provided by the embedded control system have been directly used in this study. The embedded control system also measures electric power at the generator end.

### 2.2 Experimental facility

Figure 1 is the photograph of the test facility, which shows the micro gas turbine generator system (the MGT and the generator in the upper part and the auxiliaries and the controllers in the lower part) and measuring equipments. The fuel line is located to the left of the figure. The system layout with important locations where thermodynamic parameters should be determined is shown in Fig. 2. Various temperatures and pressures as

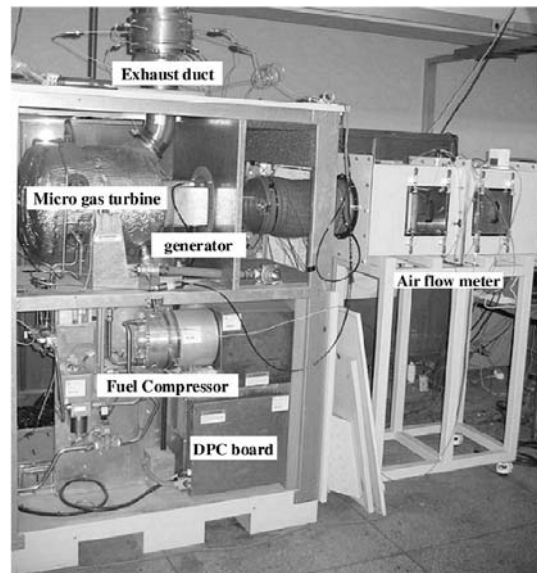


Fig. 1 Micro gas turbine test facility

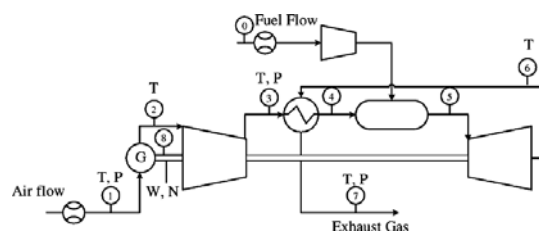


Fig. 2 Schematic of the micro gas turbine with measuring locations

well as flow rates are measured. As stated in the previous section, compressor inlet temperature ( $T_2$ ) and turbine exit temperature ( $T_6$ ) are measured by embedded thermocouples.

To analyze more detailed component performance, temperatures are additionally measured at engine inlet (point 1, before the generator), compressor exit (point 3) and engine exhaust (point 7). Three circumferentially located T-type thermocouples are used to measure the inlet temperature ( $T_1$ ). Measuring  $T_1$  and  $T_2$  gives the air temperature rise through the generator. Six K-type thermocouples are located in the exhaust duct to measure  $T_7$ . A pressure probe is equipped at the air bleed line from the compressor to measure the total pressure ( $P_3$ ) of the compressor exit air. A K-type thermocouple is inserted through the bleed line and locates at the compressor diffuser exit to measure the compressor exit temperature. Air pressure is also measured at the generator inlet ( $P_1$ ). A nozzle type air flow meter is equipped in front of the engine. The fuel flow rate is measured by a thermal mass flow meter. Table 1 summarizes the measuring quantities. Parameters at the turbine inlet (point 4) and recuperator air exit (point 5) are not measured but can be estimated by an analysis explained in the next section. In particular, estimation of these unmeasured parameters is one of the major purposes of

this study. At a designated power, measurements were carried out after the whole system reaches a sufficient steady state. Tests were performed with increment or decrement of roughly 2 kW. The measured data were saved to a PC through a data acquisition system.

### 2.3 Analysis

Ambient air enters the generator and provides its cooling. Then, the air flows into the compressor. With the measured air flow rate and temperatures at inlet and outlet of the generator ( $T_1$ ,  $T_2$ ), the shaft power is calculated using the following energy balance at the generator.

$$\dot{W}_{sh} - \dot{W}_{gen} = \dot{m}_a \cdot (h_2 - h_1) \quad (1)$$

This represents the loss at the generator. The generator efficiency is defined as follows :

$$\eta_{gen} = \frac{\dot{W}_{sh}}{\dot{W}_{gen}} \quad (2)$$

Then, the energy balance for the core engine, based on the shaft power, is as follows :

$$\dot{m}_2 h_2 + \dot{m}_f LHV_f = \dot{W}_{sh} + \dot{m}_7 h_7 \quad (3)$$

From the measurements of fuel flow rate and power, thermal efficiency based on the shaft power is calculated as follows :

$$\eta_{th} = \frac{\dot{W}_{sh}}{\dot{m}_f LHV_f} \quad (4)$$

Various measurements are used for the analysis of the component characteristic parameters. In general, the measured parameters are referred to 'performance parameters' in gas turbine diagnostics. On the other hand, parameters that produce those performance parameters, such as component efficiencies, are called 'characteristic parameters' because they represent performance characteristics of the components. Gas turbine diagnosis begins with evaluation of the characteristic parameters based on the measured performance parameters. This study also adopts a similar analysis scheme to evaluate component characteristic parameters.

The characteristic parameters that should be predicted are compressor efficiency, turbine efficiency and recuperator effectiveness. Usual definitions of the characteristic parameters are adopt-

**Table 1** List of measured parameters

Station	location	Measured parameters
0	Fuel line	Fuel flow rate
1	Inlet	Air flow rate Temperature Pressure
2	Compressor inlet	Temperature
3	Compressor exit	Temperature Pressure
4	Recuperator exit	-
5	Turbine inlet	-
6	Turbine exit	Temperature
7	Engine Exhaust	Temperature Pressure
8	Generator end	Power

ed as follows :

Compressor isentropic efficiency :

$$\eta_c = \frac{h_{3s} - h_2}{h_3 - h_2} \quad (5)$$

Turbine isentropic efficiency :

$$\eta_t = \frac{h_5 - h_6}{h_5 - h_{6s}} \quad (6)$$

Recuperator temperature effectiveness :

$$\eta_{rec} = \frac{T_4 - T_3}{T_6 - T_3} \quad (7)$$

Turbine inlet temperature ( $T_5$ ) should also be predicted together with the three component characteristic parameters. Thus, we have four parameters to determine. Simulation based analysis is used to obtain all of the unknown parameters. The usual performance simulation requires those four parameters as inputs and gives us the performance parameters as outputs. Therefore, conceptually, a reverse simulation allows us to estimate the four parameters. A similar concept has been applied to estimate major gas turbine design parameters (turbine inlet temperature, cooling flow rate as well as component efficiencies) of various heavy duty gas turbines (Kim and Ro, 1995). This scheme is also similar to the one adopted as a tool for basic performance diagnosis (Bettochi and Spina, 1999). A proven performance prediction program (Kim and Ro, 1995) is adopted as the simulation tool.

Air flow rate, compressor inlet temperature and all measured pressures (compressor inlet, compressor discharge, and exhaust) are used as given (fixed) values in the simulation. Then, the four parameters ( $\eta_c$ ,  $\eta_t$ ,  $\eta_{rec}$  and  $T_5$ ) are obtained as a result of iterative simulation to minimize the deviations between simulated and measured values of the performance parameters. First, the compressor efficiency ( $\eta_c$ ) is obtained by Eq. (5) using the measured temperatures and pressures at inlet and outlet of the compressor. Evaluation process of the remaining three parameters ( $\eta_t$ ,  $\eta_{rec}$  and  $T_5$ ) begins with assumption of the turbine inlet temperature. Turbine efficiency is obtained using assumed turbine inlet temperature ( $T_5$ ) and measured turbine exit temperature ( $T_6$ ). Using the mea-

sured turbine exit temperature ( $T_6$ ) and the recuperator gas side exit temperature ( $T_7$ , i.e. the exhaust temperature) as well as the energy balance at the recuperator, the recuperator air side exit temperature ( $T_4$ ) can be calculated. Then, Eq. (7) produces the recuperator effectiveness. Consequently, an arbitrary turbine inlet temperature results in a set of the three characteristic parameters. The simulation also gives shaft power and fuel supply rate. Then, calculated power and fuel flow are compared with those of measured values to provide the following deviations.

$$\delta_{power} = \frac{\dot{W}_{sh,sim} - \dot{W}_{sh,m}}{\dot{W}_{sh,max}} \quad (8)$$

$$\delta_{fuel} = \frac{\dot{m}_{f,sim} - \dot{m}_{f,m}}{\dot{m}_{f,max}}$$

A set of turbine inlet temperature and resulting three characteristic parameters that minimizes the following average deviation are considered to be the solution.

$$RMS = \sqrt{\frac{\delta_{power}^2 + \delta_{fuel}^2}{2}} \quad (9)$$

Miscellaneous pressure losses that cannot be measured are assumed considering design practices. Values assumed for the reference (close to design) pressure losses at the generator, recuperator air side, combustor, recuperator gas side are 0.5%, 1.0%, 4.0% and 2.0% of each inlet pressure respectively. These reference values are applied to the full power, which is close to the design point, and their variations are taken into account using a theoretical pressure loss relation (Saravanamuttoo et al., 2001).

### 3. Results and Discussion

#### 3.1 Engine performance

This paper shows results of two test cases performed at near standard ambient temperature (288K). The performance tests were carried out for the entire power range. Fig. 3 shows the ambient temperature ( $T_1$ ) and the generator exit (compressor inlet) temperature ( $T_2$ ). The ambient temperature, i.e. the generator inlet temperature, is kept

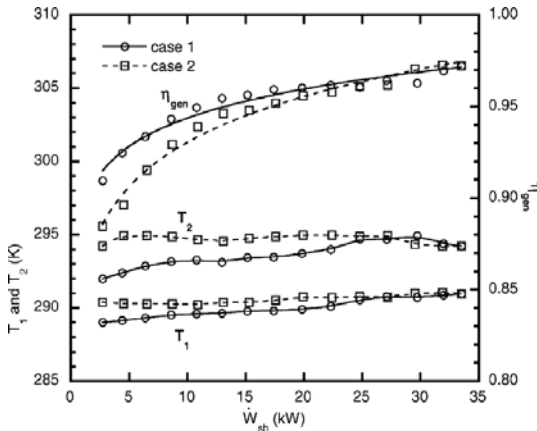


**Fig. 3** Air temperatures at generator inlet and outlet, and generator efficiency

nearly constant at around 290 K. Since the ambient temperatures of the two cases are almost same, performance results are nearly equivalent. Temperature rise at the generator is measured to be 3 to 5 K. Generator power at the full load is about 32.5 kW. Generator loss at that point is estimated to be about 1 kW. Thus, the full shaft power is estimated to be about 33.5 kW. Also shown is the generator efficiency, estimated by Eq. (2). Even though some oscillation of the data are observed, the tendency of efficiency variation conforms to general trend well enough. The generator efficiency at the full power is about 97 percent, while its value at the lowest power is about 90 percent.

Figure 4 shows the variations in the shaft speed and the compressor pressure ratio. As explained in the previous section, this engine adopts the variable speed operation. Thus, the shaft speed decreases with power. The full speed is 96,000 rpm and the lowest speed (idle speed) is 45,000 rpm. Compressor pressure ratio is slightly higher than 3.5 at the full power and about 1.4 at the lowest power. Its variation with power is nearly linear. Fig. 5 shows the variations in the air and fuel mass flow rates. With power reduction, the air flow rate decreases due to the speed reduction. Its value at the full power is measured to be about 0.284 kg/s. At the lowest power, the air flow rate is about 30% of the maximum value at the full power. The fuel flow rate decreases almost linearly with power.

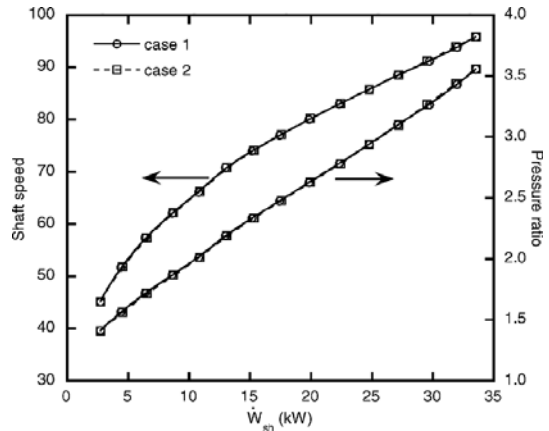


**Fig. 4** Variations in shaft speed and compressor pressure ratio with shaft power

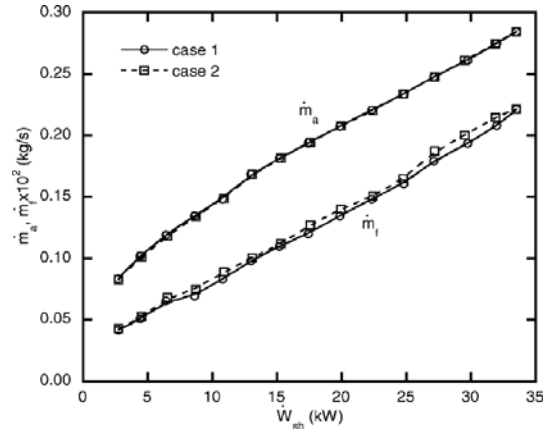


**Fig. 5** Variations in air and fuel flow rates with shaft power

Variations in measured temperatures at the turbine exit ( $T_6$ ) and engine exhaust ( $T_7$ , i.e., recuperator gas side exit) are shown in Fig. 6. Also shown is the compressor exit temperature ( $T_3$ ). The turbine exit temperature and the engine exhaust temperature at full power is 866 K and 547 K respectively. The turbine exit temperature increases almost linearly with power reduction until about 40% of the full power. It is unexpectedly high in some of the low power regime. This phenomenon has been observed repeatedly for all tests and supposed to be a result of intrinsic engine control at low load. The exhaust gas temperature decreases with power reduction. Fig. 7 shows the variation in the thermal efficiency based on

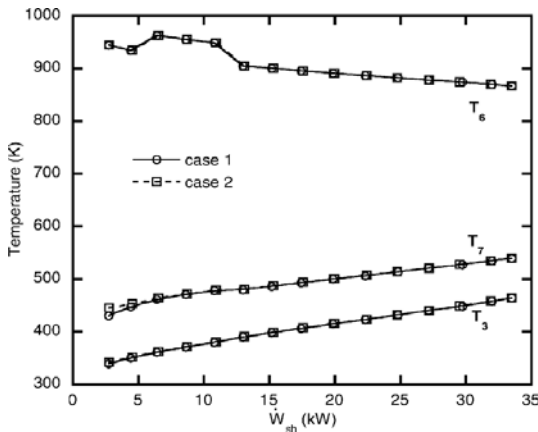


**Fig. 6** Variations in measured temperatures at turbine exit, engine exhaust (recuperator gas side exit) and compressor exit

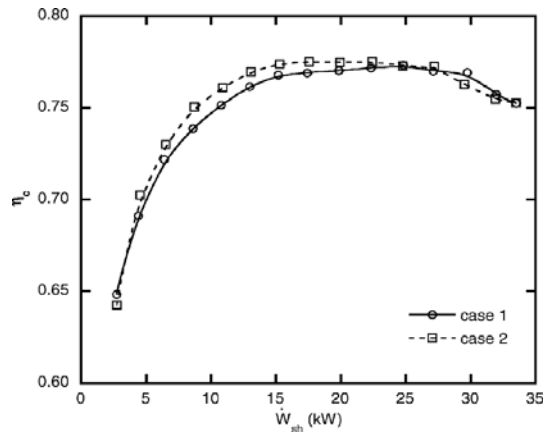


**Fig. 8** Variations in compressor efficiency with shaft power

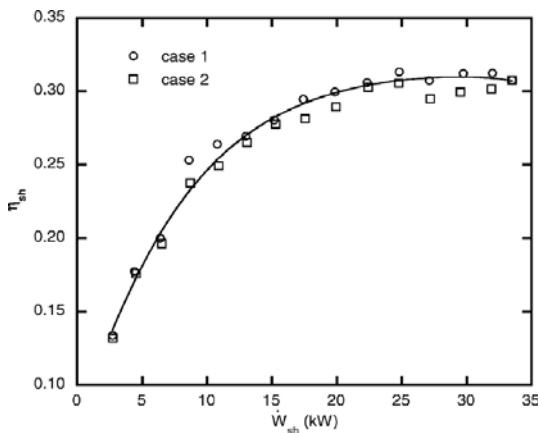


**Fig. 7** Variation in thermal efficiency of the micro gas turbine with shaft power

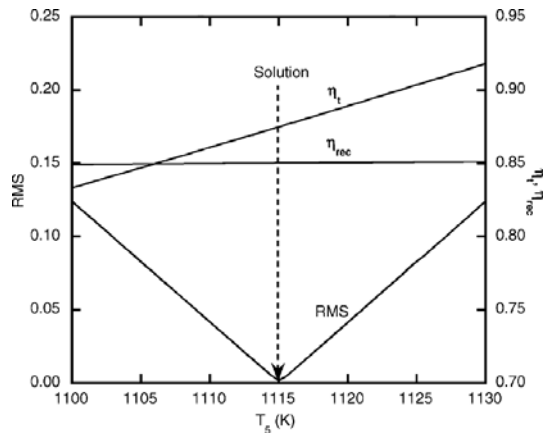


**Fig. 9** Example of the variation in the least square deviation for the full power condition of case 1

the shaft power. The efficiency at the full power is evaluated to be slightly higher than 30%. Even though there is a little scattering in the data, the variation of the efficiency conforms to the general tendency.

### 3.2 Component characteristics

Figure 8 shows the estimated compressor efficiency. At the full load, which seems to be very close to the design point, the compressor efficiency is about 75%. The compressor efficiency increases slightly with power reduction from the full load, reaches a maximum and then drops. Fig. 9 illustrates variation of the least square deviation of Eq. (9) with turbine inlet temperature in case of the full power condition of case 1 and shows the existence of the optimal solution. Also shown are the variations of the estimated recuperator effectiveness and turbine efficiency at each assumed turbine inlet temperature. There exists a clear solution that minimizes the least square deviation. The recuperator effectiveness is insensitive to the turbine inlet temperature, while the turbine efficiency varies. The estimated solution set at the optimized point is turbine inlet temperature of 1115 K, turbine efficiency of 0.875 and recuperator effectiveness of 0.85. These values seem quite reasonable considering reported design prac-

tion of Eq. (9) with turbine inlet temperature in case of the full power condition of case 1 and shows the existence of the optimal solution. Also shown are the variations of the estimated recuperator effectiveness and turbine efficiency at each assumed turbine inlet temperature. There exists a clear solution that minimizes the least square deviation. The recuperator effectiveness is insensitive to the turbine inlet temperature, while the turbine efficiency varies. The estimated solution set at the optimized point is turbine inlet temperature of 1115 K, turbine efficiency of 0.875 and recuperator effectiveness of 0.85. These values seem quite reasonable considering reported design prac-

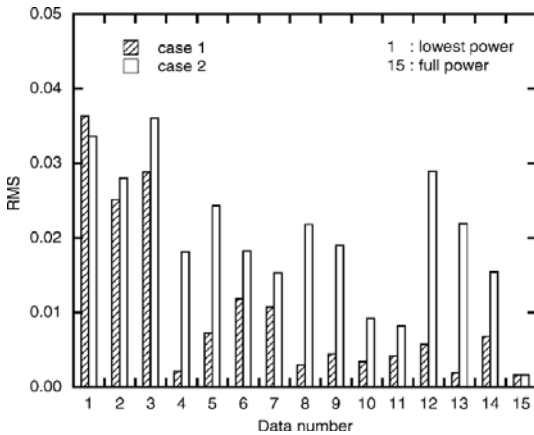


Fig. 10 Optimized average deviations for various operation conditions

tice and technology of micro gas turbines.

From the analysis mentioned above, whole sets of optimal solutions for all operating points are obtained. Fig. 10 presents the least square deviations at the optimal solution for various operating points tested. The deviation between estimation and measurement generally increases as power reduces. However, the largest deviation is less than 4 percent and two thirds of the total data are less than 2 percent.

Figure 11 shows the variation in the estimated turbine inlet temperature. TIT decreases moderately with power reduction. The abrupt increase of the measured turbine exhaust temperature shown in Fig. 6 is explained by the rise in the TIT. The decrease of TIT from the full power to the lowest power is estimated to be about 100°C. Fig. 12 presents variations in the estimated turbine efficiency. The turbine efficiency does not vary much with operating condition change.

Figure 13 shows the variation in the estimated recuperator effectiveness. The effectiveness appears to increase with power reduction. This is very reasonable because the decrease of mass flow rate results in increase of the effectiveness of a heat exchanger. The rate of effectiveness enhancement with mass flow reduction depends on the local shape and flow condition of the heat exchanger. The relation between mass flow rate and the effectiveness can be reviewed from a literature (Kim and Hwang, 2006). The variation in Fig. 13 is

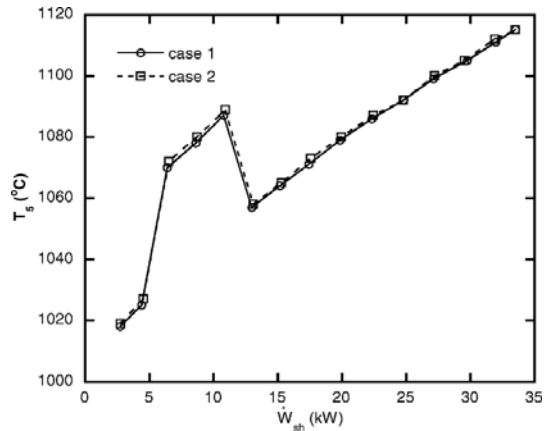


Fig. 11 Estimated turbine inlet temperature

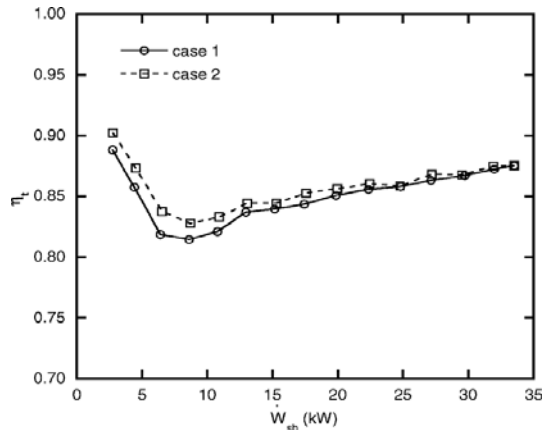


Fig. 12 Estimated turbine efficiency

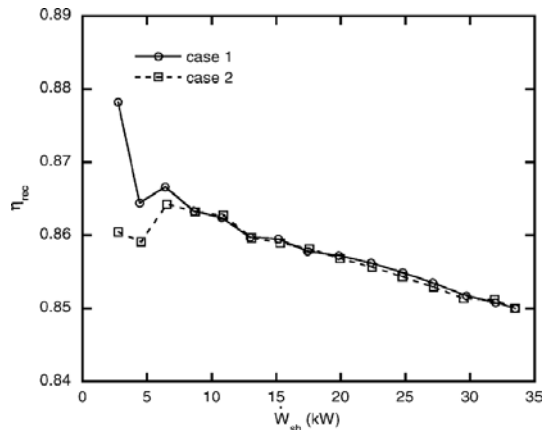


Fig. 13 Estimated recuperator effectiveness

rather moderate considering the usual theoretical laminar flow design of compact counter flow re-



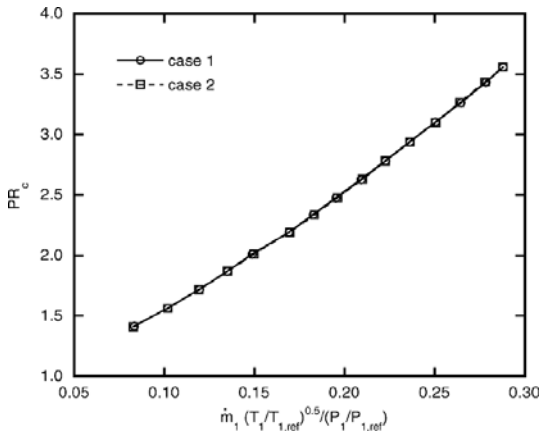


Fig. 14 Compressor running line

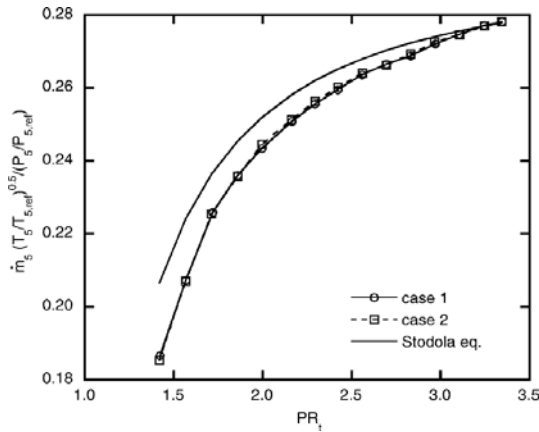


Fig. 15 Turbine running line

cuperators of primary surface type. However, the trend of the Fig. 13 confirms that the present method of predicting component characteristic parameters is sufficiently sound.

Figure 14 illustrates the compressor running line. The abscissa is the reduced mass flow. The reference compressor inlet temperature and pressure is the standard ambient condition (288 K and 101.3 kPa). Fig. 15 shows the turbine running line. The reference turbine inlet values are those at the full power conditions. Most of the operating conditions appear to be sufficiently away from the choking condition. The trend of the running line looks quite similar to the theoretical behavior described by the Stodola equation (Dixon, 1978). Thus, as a comparison, the running line predicted by the following Stodola equation is also drawn

in the figure. Subscripts 'in' and 'out' denote turbine inlet (point 5) and outlet (point 6), respectively.

$$\frac{\dot{m}_{in} \sqrt{T_{in}} / P_{in}}{(\dot{m}_{in} \sqrt{T_{in}} / P_{in})_{ref}} = \frac{\sqrt{1 - (P_{out} / P_{in})^2}}{\sqrt{1 - (P_{out} / P_{in})_{ref}^2}} \quad (10)$$

The estimated turbine operating characteristics and the curve predicted by the theoretical equation are quite similar in their shapes. Therefore, a simple equation to simulate the operating line of the current micro gas turbine is possible after a slight modification of the Stodola equation. This is very useful information in simulating the engine performance for various purposes in the future study.

### 3.3 Sensitivity of estimated characteristic parameters

Since the estimation of characteristic parameters is based on the measured parameters, the measurement accuracy, especially those of the primary parameters such as temperatures and pressure, is essential. They were checked at a static condition without running the engine by comparing with other reference temperature and pressure readings. Since the steady state conditions were measured and furthermore, serious transient effect was not observed during each measurement, the pressure measurements are believed to be sufficiently accurate. However, even at steady state, the measured temperature may possess a certain inaccuracy due to inappropriate measuring location. This may be especially important in compressor discharge temperature and the exhaust gas temperature. In measuring the compressor discharge temperature, the exact location seems to be the most important factor for an accurate measurement because several trials have showed that a slight change of the measuring location provided sensible difference in the measured temperature. At the engine exhaust, flow non-uniformity may be a source of the temperature measurement uncertainty. Therefore, influence of the accuracies of the two temperature measurements on the estimated component characteristic parameters would provide useful information for further study. The turbine exit temperature seems to be more reli-

able than the previous two temperatures because it was measured by the sensor which had been embedded by the engine manufacturer for the purpose of engine control. But, for the completeness of the error analysis, the turbine exit temperature was also included in the sensitivity analysis.

For the full power condition, the iterative analysis to obtain the component characteristic parameters were performed again with arbitrarily varied values of the three measured temperatures : turbine exit temperature (TET,  $T_6$ ), the exhaust gas temperature (EGT,  $T_7$ ) and the compressor discharge temperature (CDT,  $T_3$ ). Only single

effects of each measurement is examined (all the other temperatures except the designated temperature were kept at the measured values). Variations within 10 K (both positive and negative changes) were examined. Sensitivities of the compressor efficiency, the turbine inlet temperature, the turbine efficiency and the recuperator effectiveness to the measured temperatures are shown in Figs. 16 to 19, respectively. Each figure presents influences of three temperatures on each estimated parameter. Fig. 16 confirms that the compressor efficiency is obtained only by measured CDT without the iterative estimation (refer to 2.3). Thus,

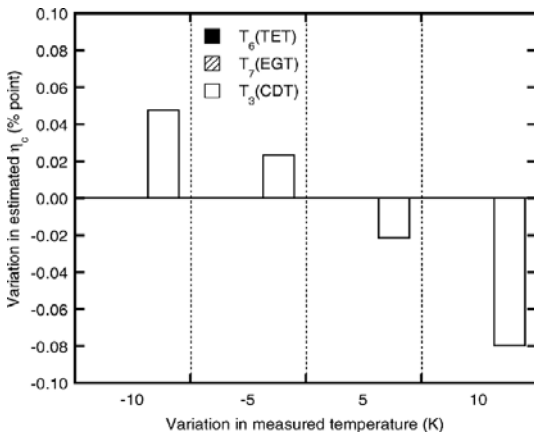


**Fig. 16** Sensitivity of estimated compressor efficiency to measured temperatures at the full power condition of case 1

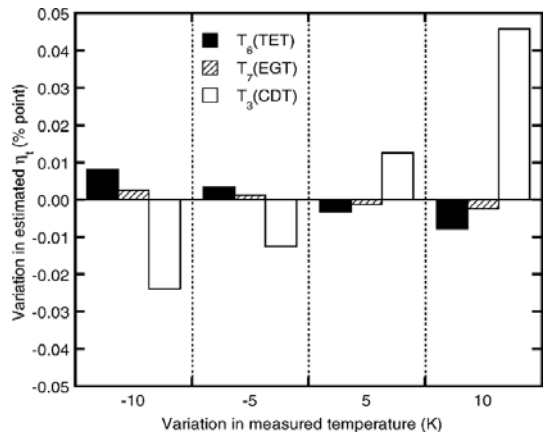


**Fig. 18** Sensitivity of estimated turbine efficiency to measured temperatures at the full power condition of case 1

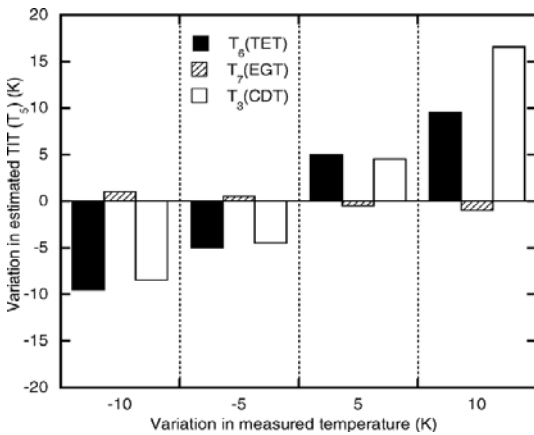


**Fig. 17** Sensitivity of estimated turbine inlet temperature to measured temperatures at the full power condition of case 1

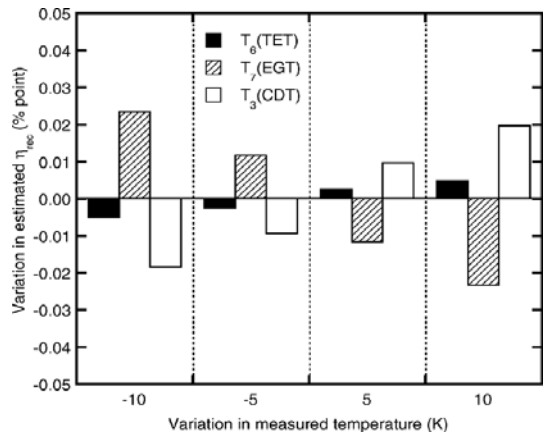


**Fig. 19** Sensitivity of estimated recuperator effectiveness to measured temperatures at the full power condition of case 1

it is not affected by the other two temperatures (TET and EGT). Only 10 K higher measurement of CDT would cause 8 percent point decrease of the predicted compressor efficiency. Then, assuming this new value of CDT, we get 67% compressor efficiency. This seems to be very low considering current state-of-the-art centrifugal compressor design practice. Therefore, the original CDT, leading to compressor efficient of 75%, or a rather lower CDT, providing a better efficiency, would be more feasible. The CDT measurement also affects all of the other estimated quantities much. If CDT is higher (thus, compressor efficiency is lower), the other components are predicted to operate with better performance (higher TIT,  $\eta_t$ ,  $\eta_{rec}$ ) in order to satisfy the given engine performance by compensating for the lower compressor performance. 10 K higher CDT provides about 4.5 percent point increase of the estimated turbine efficiency. Then, the new estimated turbine efficiency would be 92%, which does not seem very appropriate as a radial turbine efficiency. Thus, we can again confirm that CDTs that are higher than currently measured value is not very reliable. A higher TET predicts a higher TIT, but does not affect much the other two parameters ( $\eta_t$ ,  $\eta_{rec}$ ). A higher EGT predicts a lower recuperator effectiveness. Its correlation with other two parameters (TIT,  $\eta_t$ ) is very weak. In conclusion, the compressor discharge temperature affects the estimated quantities most widely, and thus its accurate measurement is very important.

#### 4. Conclusions

This study has analyzed engine performance and component characteristics of a micro gas turbine. Results are summarized as follows.

(1) With the measurement of the generator loss, the net power from the micro gas turbine shaft was isolated, which allowed accurate analysis of the core engine. The estimated generator efficiency conforms to the general tendency.

(2) An analysis method, which is based on optimal matching of simulated data to measure performance data and predicts turbine inlet tem-

perature and component characteristic parameters such as compressor efficiency, turbine efficiency, recuperator effectiveness, was developed. Those parameters for the entire operation range were successfully obtained.

(3) The estimated turbine inlet temperature and three characteristic parameters are quite reasonable. The predicted behaviors of the characteristic parameters with operating condition change were also reasonable, which validates the method to obtain those parameter adopted in this study. In particular, increase of the recuperator effectiveness with reducing mass flow was predicted and the turbine running line was close to that predicted by a theoretical equation. This analysis scheme can further be extended to performance diagnosis of the micro gas turbine.

(4) Sensitivities of estimated parameters to the accuracies of the measured temperatures were analyzed. The compressor discharge temperature affects the estimated quantities most widely, and thus its accurate measurement is very important.

#### Acknowledgments

This work was supported by the grant from ETEP funded by MOCIE of Korea.

#### References

- Bettocchi, R. and Spina, P. R., 1999, "Diagnosis of Gas Turbine Operating Conditions by Means of the Inverse Cycle Calculation," ASME paper 99-GT-185.
- Chiang, H. D., Wang, C. and Hsu, C., 2004, "Performance Testing of a Microturbine Generator Set with Twin Rotating Disk Regenerators," ASME paper GT2004-53467.
- Davison, C. R. and Birk, A. M., 2004, "Steady State and Transient Modeling of a Micro-Turbine with Comparison to Operating Engine," ASME paper GT2004-53378.
- Dixon, S. L., 1978, *Fluid Mechanics, Thermodynamics of Turbomachinery*, 3rd ed., Pergamon Press.
- Kim, T. S. and Hwang, S. H., 2006, "Part Load Performance Analysis of Recuperated Gas Tur-

bines Considering Engine Configuration and Operation Strategy,” *Energy*, Vol. 31, pp. 260~277.

Kim, T. S. and Ro, S. T., 1995, “Comparative Evaluation of the Effect of Turbine Configuration on the Performance of Heavy-duty Gas Turbines,” ASME paper 95-GT-334.

Lee, J. H. and Kim, T. S., 2006, “Analysis of Design and Part load Performance of Micro Gas Turbine/Organic Rankine Cycle Combined Systems,” *J. of Mechanical Science and Technology*, Vol. 20, pp. 1502~1513.

McDonald, C. F., 2000, “Low-cost Compact Primary Surface Recuperator Concept for Microturbines,” *Applied Thermal Engineering*, Vol. 20, pp. 471~497.

McDonald, C. F. and Rodgers, C., 2005, “Ceramic Recuperator and Turbine—The Key to Achieving a 40 Percent Efficient Microturbine,” ASME paper GT2005-68644.

Rodgers, C., Watts, J., Thoren, D., Nichols, K., Brent, R., 2001, *Microturbines*, In : Borbely, A.M. and Kreider, J. F., editors. *Distributed Genera-*

*tion*, New York, CRC Press, pp. 119-150.

Saravanamuttoo, H. I. H., Cohen, H. and Rogers, G. F. C., 2001, *Gas Turbine Theory*, 5th ed., John Wiley & Sons.

Shibata, R., Nakayama, Y., Machiya, S. and Kobayashi, K., 2003, “The Development of 300 kW Class High Efficiency Micro Gas Turbine “RGT3R”,” Proc. of the Int. Gas Turbine Congress, Nov. 2-7, 2003, Tokyo, Japan, IGTC2003 Tokyo TS-115.

Simon, T. W. and Jiang, N., 2003, “Micro- or Small Gas Turbines,” Proc. of the Int. Gas Turbine Congress, Nov. 2-7, 2003, Tokyo, Japan, IGTC2003Tokyo KS-1.

U.S. Department of Energy, 2000, *Advanced Microturbine Systems, Program Plan for Fiscal Year 2000 through 2006*.

Yin, J., Li, M. S., Huang, W., 2003, “Performance Analysis and Diagnostics of a Small Gas Turbine,” Proc. of the Int. Gas Turbine Congress, Nov. 2-7, 2003, Tokyo, Japan, IGTC2003Tokyo TS-006.